Eur. Phys. J. Plus (2017) **132**: 455
DOI 10.1140/epjp/i2017-11725-0

THE EUROPEAN PHYSICAL JOURNAL PLUS

Regular Article

Construction of the energy matrix for complex atoms*

Part VIII: Hyperfine structure HPC calculations for terbium atom

Magdalena Elantkowska[1,a], Jarosław Ruczkowski[2], Andrzej Sikorski[2], and Jerzy Dembczyński[2]

[1] Institute of Materials Research and Quantum Engineering, Faculty of Technical Physics, Poznan University of Technology, Piotrowo 3, 60-965 Poznań, Poland
[2] Institute of Control, Robotics and Information Engineering, Faculty of Electrical Engineering, Poznan University of Technology, Piotrowo 3A, 60-965 Poznań, Poland

Received: 10 August 2017 / Revised: 13 September 2017
Published online: 3 November 2017

Abstract. A parametric analysis of the hyperfine structure (hfs) for the even parity configurations of atomic terbium (Tb I) is presented in this work. We introduce the complete set of $4f^N$-core states in our high-performance computing (HPC) calculations. For calculations of the huge hyperfine structure matrix, requiring approximately 5000 hours when run on a single CPU, we propose the methods utilizing a personal computer cluster or, alternatively a cluster of Microsoft Azure virtual machines (VM). These methods give a factor 12 performance boost, enabling the calculations to complete in an acceptable time.

1 Introduction

The present paper is the eighth one in the series of our methodological approach regarding the atomic structure calculations. Six previously published papers, under the common title *Construction of the energy matrix for complex atoms*, contain a description of our method for semi-empirical analysis of complex electronic systems in multiconfiguration approximation up to the second order of the perturbation theory [1–6]. The seventh paper [7] of the above-mentioned cycle was the application of our many-body parametrization method to analyze fine structure in 4f- and 5f-shell atoms.

The choice of the investigated element was caused by a new experimental data of the hyperfine structure splitting of the atomic terbium levels obtained by our experimental group [8–11]. Within the work [10] the fine- and hyperfine structure analysis of seven even-parity configurations of Tb I ($4f^85d^3$, $4f^85d^26s$, $4f^85d6s^2$, $4f^96s6p$, $4f^96s7p$, $4f^96s8p$, $4f^95d6p$) was performed. The calculations were carried out in limited basis states, it means for $4f^8$-core to 13 terms and for $4f^9$-core to 3 terms.

After applying of novelty type of optimizing calculation procedures we were able to repeat the fine structure (fs) analysis for terbium atom in a full number of $4f^8$ and $4f^9$-core states and the results were described in the aforementioned paper [7]. The huge energy matrix of the configuration system under consideration contained 74418 possible energy levels. The size of the largest submatrix, for $J = 9/2$, was 9936. The results of the fine structure calculations obtained within paper [7] compared to those published earlier [10] conducted with the restricted $4f^N$core, were definitely better. In the fine structure least-squares fit we achieved mean error for energy levels values of $\sigma(E) = 37\,\mathrm{cm}^{-1}$ (old value was $\sigma(E) = 56\,\mathrm{cm}^{-1}$). We used 99 known experimental even-parity energy levels and 26 fitted parameters. The description of the levels above $17000\,\mathrm{cm}^{-1}$ based on comparison with experimental g_j-Landé factors seemed to be correctly determined. However, the confirmation of the obtained levels designation could be possible after the performing of the hyperfine structure parameterization in the same, complete basis states.

Therefore, in the current article we are reporting the results of the hyperfine structure analysis in the full number of $4f^8$ and $4f^9$-core states, abandoning the previous limitations. Such huge hyperfine structure calculations have not been presented in literature so far.

* Supplementary material in the form of a .pdf file available from the Journal web page at
https://doi.org/10.1140/epjp/i2017-11725-0

[a] e-mail: magdalena.elantkowska@put.poznan.pl

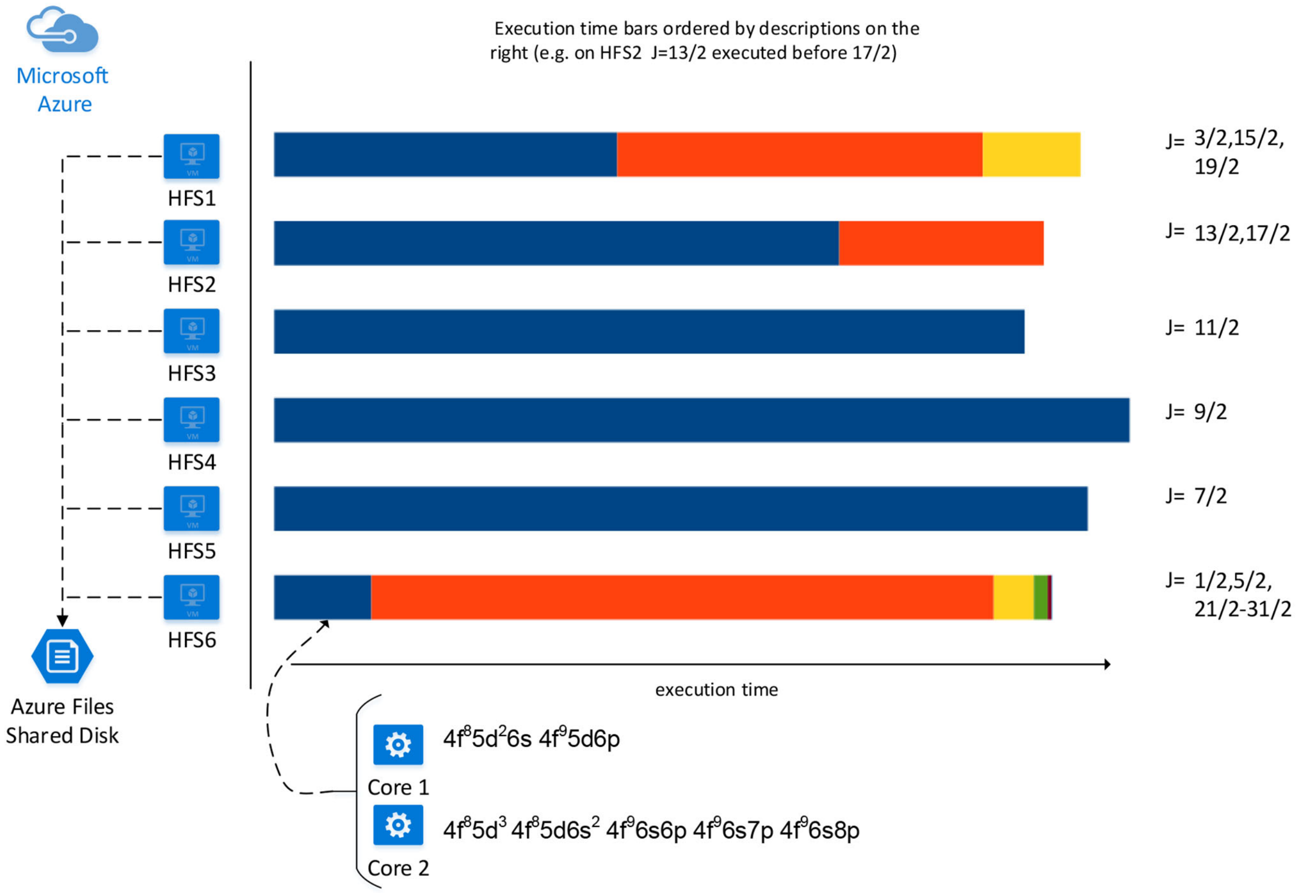

Fig. 1. Computation of each J is assigned to a DS11v2 - 2 cores - Azure VM in a way to minimize the total execution time, now dominated by the $J = 9/2$ submatrix. Running the calculations on 6 VMs 2 cores each resulted in 12 times performance boost. In this version, the electronic configurations are statically assigned to two threads. One thread calculates $4f^8 5d^2 6s$, $4f^9 5d6p$, the other one $4f^8 5d^3$, $4f^8 5d6s^2$, $4f^9 6s6p$, $4f^9 6s7p$, $4f^9 6s8p$.

The next section of this paper contains the details of computational procedures optimization. The results of fine- and hyperfine structure many-body parametrization method for the even configurations system of terbium atom are presented in sect. 3.

2 Computing hfs angular coefficients with Azure HPC infrastructure

At least two levels of parallel computation are possible and desired as the calculating angular coefficient is a time consuming process. One level is straightforward as the underlying Hamiltonian is block diagonal with respect to J. In consequence, the individual blocks can be processed independently. This independence allows distribution of the computation among multiple nodes as there are no interactions, except the final barrier when the calculations for all J complete. At J block level of parallelism, this property makes our computation location transparent as each J block can be assigned to a designated thread or to a separate node. Note, that distributing the computation among multiple nodes results in better scalability and requires only allocating an appropriate number of nodes (in our case six Azure VMs —fig. 1).

The second level of parallelism is more subtle and requires some care. There are multiple (*i.e.* 8 in the case of odd configurations of atomic terbium) configurations within each J which can also be computed concurrently, but now the dependencies between partial results are present as the parameters from all concurrently processed configurations must be ordered to produce properly structured data which is subsequently used as an input for hfs fitting. There are two phases of the calculations at the electronic configuration level: the first, more time-consuming phase computes the coefficients resulting from internal interactions, the second (much shorter) computes the inter-configuration part, hence a barrier must be present to co-ordinate the execution. When a thread calculating individual configuration reaches the barrier, it blocks until all other configurations complete and then the angular coefficients are ordered and the final phase, which calculate inter-configuration interactions is executed. As this final phase is relatively fast, it is assigned to a single thread.

The main factor affecting the computation time for a single configuration can be estimated from the rules of total angular momentum coupling which determine the base size. The other factor is the number of parameters which, however, is known in advance (this is simply our input). With these two factors available one can easily forecast the execution time needed to process each configuration and allocate the resources, assigning individual configurations to computational nodes in a way that results in an approximately optimal execution. Observe, that on a single CPU the total execution time would equal the sum of bars lengths in fig. 1. Despite this significant performance boost, in our future work we are going to present a solution that allows full scalability, *i.e.* the optimal utilization of an arbitrary number of cores.

3 Results of the semi-empirical approach

In our earlier paper on Tb I [10] we investigated the atomic structure of 7 even-parity configurations system using a semi-empirical parametrization method, taking into account electromagnetic interactions up to the second-order perturbation theory. The fine structure angular coefficient matrices for the multiconfiguration system, listed in the introduction, necessary for the least-squares fitting program, were constructed with the use of our computer code. The calculations were restricted to the lowest lying states of $4f^8$- and $4f^9$-core. The contributions from the second-order perturbation theory concerning the configuration interaction (CI) effects, electrostatically correlated spin-orbit interactions (CSO), as well as electrostatically correlated hyperfine interactions (CHFS), described in the series [1–6], were possible to a limited extent only. The CI effects of two-electron excitations were included in the consideration by adding the term $\alpha L(L+1)+\beta S(S+1)$, according to [12,13] and [14]. For the CSO interactions only the excitations of one electron from closed n_0d^{10} shells into an open 5d-shell were taken into consideration. For the CHFS interactions, the excitations of one electron from closed n_0s shells to empty n's shells or to an open 6s-shell were taken into account. A detailed description of our approach of the fine- and hyperfine structure analysis of Tb I was presented by us in sect. 4 in paper [10] and the final results of the semi-empirical calculations were summarized in four tables. The values of the intra-configuration and inter-configuration fs radial parameters were contained in tables 3 and 4, respectively. A comparison of the experimental and calculated energy values and hfs A and B constants were given in table 5. The values of the one- and two-body hyperfine structure parameters were presented in table 6. These values should be compared with new results obtained by the precise studies carried out within the framework of this work.

The current results of the semi-empirical fine- and hyperfine structure analysis of the even levels of the neutral terbium atom are presented in tables 1–5.

The values of radial fine structure parameters, their statistical errors and the values obtained with the COWAN CODE [15,16] (HFR) are given in tables 1 and 2. The second-order contributions concerning electrostatically correlated spin-orbit interactions were included according to the procedure described in the work [5]. This means that the excitations of one electron from open $4f^8$-, $4f^9$-shells to empty n′f shells, the excitations of one electron from closed n_0d^{10} shells into an open 5d-shell and the excitations of one electron from closed n_0p^6 shells into an open 6p-shell, were taken into account.

The comparison of the experimental and calculated energy values and hfs A and B constants is shown in table 3. The complete version of this table, together with the predictions of the energy values and hfs constants for the levels up to approximately $28000\,\mathrm{cm}^{-1}$ is presented in supplementary material associated with this paper.

In our procedure, we used all the experimental data known so far, *i.e.*, the values of 99 energy electronic levels, g_j-Landé factors known for 66 energy levels 86 A and 84 B hyperfine structure constants. The energy and g_J values were taken from the NIST Atomic Spectra Database [17], which is based primarily on the monograph of Martin *et al.* [18]. The experimentally determined hfs constants were taken from Childs [19–21], Furmann [8,9] and Stefanska [10,22]. In the fs-fit with 369 parameters, 24 of which were treated as free, we achieved a mean-square deviation of $37\,\mathrm{cm}^{-1}$.

The first three columns in the table 3 present the values of experimental, calculated energy of electronic levels and the difference between them in cm^{-1}. The two main fine structure components with their percentages, are given in columns 4–7. In next columns, the calculated g_J values are compared with the experimental ones. In columns 10 and 12 the experimental hyperfine constants A and B are listed together with their experimental uncertainties. The calculated A and B constants for all energy levels are listed in columns 11 and 13. We achieved mean errors for A constants $\sigma(A) = 17\,\mathrm{MHz}$ and for B constants $\sigma(B) = 36\,\mathrm{MHz}$, respectively.

The hfs constants A and B for the energy levels in region about $23000\,\mathrm{cm}^{-1}$ were very helpful in the identification of J-quantum numbers and assignment of the spectroscopic description. The semi-empirical calculations of the hyperfine constants A and B showed that it was possible to clarify the configuration and designation of the energy levels in a wide energy range.

The comparison of the experimental and calculated hfs A and B constants [MHz] of the even-parity levels obtained in full and limited number of $4f^8$ and $4f^9$-core states is contain in table 4.

Table 1. Values of the intra-configuration fine structure parameters (cm^{-1}); (*) denotes an fixed parameter, ^{a} denotes arbitrarily assumed value of the center of gravity of the configuration.

Parameter	Value		HFR
even configurations			
$E_{AV}(4f^8 5d^3)$	103528	(*)	104681
$F^2(4f,4f)$	93725	(*)	95180
$F^4(4f,4f)$	69409	(*)	59681
$F^6(4f,4f)$	35223	(192)	42927
$F^2(5d,5d)$	22334	(*)	22670
$F^4(5d,5d)$	13010	(*)	14237
$F^2(4f,5d)$	15274	(80)	14605
$F^4(4f,5d)$	10692	(127)	6631
$G^1(4f,5d)$	6228	(80)	6388
$G^3(4f,5d)$	8407	(194)	5004
$G^5(4f,5d)$	7386	(173)	3768
$\zeta(4f)$	2117	(14)	1768
$\zeta(5d)$	386	(42)	699
$E_{AV}(4f^8 5d^2 6s)$	84320	(104)	84320^a
$G^2(5d,6s)$	14692	(194)	13902
$G^3(4f,6s)$	2001	(54)	1119
$\alpha(4f^8 5d^2 6s)$	4	(1)	
$\beta(4f^8 5d^2 6s)$	279	(7)	
$R^0(4f4f,4fn'f)\zeta(4f,n'f)$	14	(*)	
$R^2(4f4f,4fn'f)\zeta(4f,n'f)$	329	(*)	
$D^0(4f5d,n'f5d)\zeta(4f,n'f)$	-1	(*)	
$D^2(4f5d,n'f5d)\zeta(4f,n'f)$	-65	(*)	
$E^1(4f5d,5dn'f)\zeta(4f,n'f)$	-206	(*)	
$R^2(n_0d5d,5d5d)\zeta(n_0d,5d)$	668	(*)	
$D^0(n_0d6s,5d6s)\zeta(n_0d,5d)$	32	(8)	
$E^2(n_0d6s,6s5d)\zeta(n_0d,5d)$	-36	(*)	
$D^2(n_0d4f,5d4f)\zeta(n_0d,5d)$	-255	(*)	
$E^1(n_0d4f,4f5d)\zeta(n_0d,5d)$	-352	(22)	
$E_{AV}(4f^8 5d6s^2)$	69348	(80)	72896
$\alpha(4f^8 5d6s^2)$	8	(1)	
$\beta(4f^8 5d6s^2)$	333	(6)	
$E_{AV}(4f^9 6s6p)$	74000	(115)	82827
$F^2(4f,6p)$	1904	(*)	2508
$G^1(6s,6p)$	12612	(295)	17375
$G^2(4f,6p)$	710	(*)	562
$G^4(4f,6p)$	520	(*)	490
$\zeta(6p)$	1796	(43)	1344
$E^2(4f6p,6pn'f)\zeta(4f,n'f)$	-238	(*)	
$E^1(n_0p6s,6s6p)\zeta(n_0p,6p)$	103	(*)	
$\alpha(4f^9 6s6p)$	13	(4)	
$\beta(4f^9 6s6p)$	27	(12)	
$E_{AV}(4f^9 6s7p)$	96978	(*)	100815
$E_{AV}(4f^9 6s8p)$	104241	(*)	110007
$E_{AV}(4f^9 5d6p)$	92517	(*)	100648
$F^2(5d,6p)$	10021	(*)	10021
$G^1(5d,6p)$	8564	(*)	8564
$G^3(5d,6p)$	5518	(*)	5518

Table 2. Values of configuration interactions radial parameters (cm^{-1}); (*) denotes a fixed parameter, (**) represents the same as the first parameter in the table.

Configurations	Parameter	Value		HFR
even configurations				
$4f^85d^3 \leftrightarrow 4f^85d^26s$	R^2(5d5d,5d6s)	−8516	(170)	−15876
	D^2(4f5d,4f6s)	−1403	(*)	−861
	E^3(4f5d,6s4f)	−2312	(*)	892
$4f^85d^26s \leftrightarrow 4f^85d6s^2$	R^2(5d5d,5d6s)	−8516	(**)	−16491
	D^2(4f5d,4f6s)	−1403	(*)	−769
	E^3(4f5d,6s4f)	−2312	(*)	1044
$4f^85d^3 \leftrightarrow 4f^85d6s^2$	R^2(5d5d,6s6s)	15431	(*)	15431
$4f^85d^26s \leftrightarrow 4f^96s6p$	R^1(5d5d,4f6p)	−1388	(*)	2700
	R^3(5d5d,4f6p)	863	(*)	742
$4f^85d^3 \leftrightarrow 4f^95d6p$	R^1(5d5d,4f6p)	2700	(*)	2912
	R^3(5d5d,4f6p)	742	(*)	783
$4f^85d6s^2 \leftrightarrow 4f^96s6p$	D^1(5d6s,4f6p)	−3610	(*)	−5555
	E^3(5d6s,6p4f)	−7301	(*)	−998
$4f^85d^26s \leftrightarrow 4f^95d6p$	D^1(5d6s,4f6p)	−3610	(*)	−4682
	E^3(5d6s,6p4f)	−7301	(*)	−1148
$4f^96s6p \leftrightarrow 4f^96s7p$	E^1(6s6p,7p6s)	5602	(*)	5602
	D^2(4f6p,4f7p)	1012	(*)	1012
	E^2(4f6p,7p4f)	260	(*)	260
	E^4(4f6p,7p4f)	227	(*)	227
	ζ(6p,7p)	350	(*)	
$4f^96s6p \leftrightarrow 4f^95d6p$	D^2(6s6p,5d6p)	−11347	(*)	−11347
	E^1(6s6p,6p5d)	−12107	(*)	−12107
	D^2(4f6s,4f5d)	−1431	(*)	−1431
	E^3(4f6s,5d4f)	679	(*)	679

In our published earlier paper [10], following Sandars and Back theory [23] we used the one-body radial parameters $a_{nl}^{\kappa k}$, $b_{nl}^{\kappa k}$, where $\kappa k = 01, 12$ for magnetic-dipole hfs interactions and $\kappa k = 02, 11, 13$ for electric-quadrupole hfs interactions. The contributions from the second-order perturbation theory, so-called electrostatically correlated hyperfine interactions, concerned with the excitations of one electron from closed shells to an open shell: $n_0s \rightarrow 5d$, $n_0d \rightarrow 5d$ and from an open 4f-shell to empty n′f shells dependent on $\kappa k = 01, 12$ or 02 were omitted. The above restrictions were made due to the huge size of the hyperfine structure matrix. Only "hfs core-polarization effects", *i.e.* the influence of the excitations of electrons from closed n_0s shells to empty n′s shells or to an open 6s-shell on the hyperfine structure, were taken into account.

The optimization of our computer procedures for generating the angular coefficient of the hyperfine structure matrix presented within this work, allowed the quantitative determination of one- and two-body contributions to the hyperfine structure.

The values of the one- and two-body hyperfine structure parameters (MHz) and effective radial integrals (a.u.) obtained from the experimental data for the even parity configurations of Tb I are include in table 5. The ratio of the one- and two-body parameters $\kappa k = 12$ and $\kappa k = 01$ was assumed to amount to 1. For the parameters including electrostatic integrals of the order $t = 4$ the ratio in relation to corresponding $t = 2$ parameters were set to 0.65071 (from Hartree-Fock calculations [24]). The contributions originating on excitations from closed n_0d shells to an open 5d-shell and from an open 4f-shell to empty n′f shells dependent on $\kappa k = 01, 12$ or 02 were specified. As we wrote in our earlier works [6, 10, 25], in Sandars and Beck theory [23] the operator **s** and the radial parameter a_{nl}^{10} (where $l > 0$) represent relativistic effects in the hyperfine structure. In our method we assume that the parameter a_{nl}^{10} for $l > 0$ is equal to zero. We can make this assumption because, according to, *e.g.*, Feneuille and Armstrong [26], Armstrong [27] and Lindgren and Morrisson [28] the relativistic effects and configuration interaction effects, concerning the excitation of electrons from the closed shells to the empty shells, have the same angular part. Thus, the above mentioned effects are inseparable and is not possible to determine those values independently in the least-squares procedure by use a_{nl}^{10} radial parameter.

Table 3. Comparison of the experimental and calculated energy values (cm^{-1}) and hfs A and B constants (MHz) for even-parity configuration system of Tb I. The comlete version of this table, together with the predictions of the energy values and hfs constants for the levels up to approximately 28000 cm^{-1} is presented in supplementary material associated with this paper.

E_{exp}	E_{calc}	ΔE	%	Main comp.	%	Sec. comp.	$g_{J_{calc}}$	$g_{J_{exp}}$	A_{exp}		A_{calc}	B_{exp}		B_{calc}	Ref.
$J = 1/2$															
4018.210	4099	−81	86.9	$4f^8(^7F)5d6s^2\,^8G$	3.1	$4f^8(^5D)5d6s^2\,^6F$	−1.156	−1.191	2584.8	(4.0)	2591				[19]
6259.090	6189	70	85.9	$4f^8(^7F)5d6s^2\,^8F$	3.0	$4f^8(^5D)5d6s^2\,^6D$	3.806	3.840	−1762.5	(8.9)	−1797				[10]
$J = 3/2$															
3705.820	3759	−53	79.8	$4f^8(^7F)5d6s^2\,^8G$	8.5	$4f^8(^7F)5d6s^2\,^8F$	1.044	1.022	883.905	(0.030)	884	−15.510	(0.250)	−16	[19]
5483.980	5486	−2	41.7	$4f^8(^7F)5d6s^2\,^8F$	40.3	$4f^8(^7F)5d6s^2\,^8D$	2.252	2.320	−177.8	(7.6)	−159	−504	(23)	−518	[10]
6849.720	6893	−43	48.0	$4f^8(^7F)5d6s^2\,^8D$	37.8	$4f^8(^7F)5d6s^2\,^8F$	2.378	2.335	−755.3	(5.2)	−749	281	(16)	325	[10]
8336.310	8341	−5	82.9	$4f^8(^7F)5d6s^2\,^8H$	4.4	$4f^8(^7F)5d6s^2\,^6G$	−0.343	−0.360	1645.9	(4.5)	1644	744	(25)	778	[10]
	10754		75.6	$4f^8(^7F)5d6s^2\,^6F$	5.1	$4f^8(^7F)5d6s^2\,^6G$	1.045				919			251	
10920.180	10882	38	77.4	$4f^8(^7F)5d^26s\,^{10}G$	8.0	$4f^8(^7F)5d^26s\,^{10}G$	2.149	2.145	1001.8	(3.2)	1001	−133	(19)	−123	[10]
$J = 5/2$															
3174.575	3189	−14	67.1	$4f^8(^7F)5d6s^2\,^8G$	17.5	$4f^8(^7F)5d6s^2\,^8F$	1.373	1.355	652.766	(0.020)	652	267.611	(0.150)	267	[19]
4695.505	4709	−14	48.6	$4f^8(^7F)5d6s^2\,^8D$	22.4	$4f^8(^7F)5d6s^2\,^8F$	1.805	1.831	215.653	(0.015)	211	−401.862	(0.060)	−420	[19]
6801.190	6815	−14	47.2	$4f^8(^7F)5d6s^2\,^8F$	33.1	$4f^8(^7F)5d6s^2\,^8D$	1.808	1.800	−123.7	(2.8)	−113	−286	(15)	−290	[10]
8130.680	8124	7	80.2	$4f^8(^7F)5d6s^2\,^8H$	5.0	$4f^8(^7F)5d6s^2\,^6G$	0.715	0.705	874.4	(4.8)	875	411	(25)	433	[10]
10030.350	10031	−1	69.9	$4f^8(^7F)5d6s^2\,^6F$	7.8	$4f^8(^7F)5d6s^2\,^6G$	1.297	1.305	783.5	(0.1)	737	515.4	(9.7)	546	[8]
10456.670	10414	43	70.0	$4f^8(^7F)5d^26s\,^{10}G$	11.4	$4f^8(^7F)5d^26s\,^{10}F$	1.802	1.800	912.9	(6.9)	907	149	(35)	105	[10]
	11569		62.0	$4f^8(^7F)5d6s^2\,^6G$	7.9	$4f^8(^7F)5d6s^2\,^6D$	0.959				756			107	
	11919		79.5	$4f^8(^7F)5d6s^2\,^8P$	3.3	$4f^8(^7F)5d6s^2\,^8D$	2.233				−613			359	
12296.45	12243	53	49.2	$4f^8(^7F)5d6s^2\,^6D$	17.1	$4f^8(^7F)5d6s^2\,^6P$	1.613		332.6	(0.4)	288	−52	(24)	−26	[10]
$J = 7/2$															
2419.480	2402	18	51.0	$4f^8(^7F)5d6s^2\,^8G$	25.8	$4f^8(^7F)5d6s^2\,^8F$	1.487	1.477	591.564	(0.007)	588	733.233	(0.070)	721	[19]
3819.850	3840	−20	47.4	$4f^8(^7F)5d6s^2\,^8D$	28.2	$4f^8(^7F)5d6s^2\,^8G$	1.631	1.642	358.918	(0.007)	355	−140.881	(0.050)	−157	[19]
6488.280	6473	16	51.5	$4f^8(^7F)5d6s^2\,^8F$	21.3	$4f^8(^7F)5d6s^2\,^8D$	1.638	1.635	114.9	(0.3)	116	−498.7	(0.7)	−531	[8]
7839.850	7817	23	75.9	$4f^8(^7F)5d6s^2\,^8H$	6.2	$4f^8(^7F)5d6s^2\,^6G$	1.071	1.050	606.2	(0.7)	623	429.7	(0.4)	419	[8]
8994.660	9007	−12	61.0	$4f^8(^7F)5d6s^2\,^6F$	13.0	$4f^8(^7F)5d6s^2\,^6D$	1.406	1.414	710.991	(0.003)	696	966.850	(0.003)	987	[21]
9867.650	9830	38	61.8	$4f^8(^7F)5d^26s\,^{10}G$	16.5	$4f^8(^7F)5d^26s\,^{10}F$	1.683	1.680	903.5	(2.5)	898	533	(23)	483	[10]
10324.740	10304	21	63.0	$4f^8(^7F)5d6s^2\,^8P$	13.5	$4f^8(^7F)5d6s^2\,^6P$	1.853	1.916	−35.1	(2.0)	−16	−563.3	(8.5)	−393	[8]
	10498		25.0	$4f^8(^7F)5d6s^2\,^6D$	22.3	$4f^8(^7F)5d6s^2\,^6P$	1.534				474			400	
11107.07	11092	15	43.0	$4f^8(^7F)5d6s^2\,^6G$	16.1	$4f^8(^7F)5d6s^2\,^6F$	1.275		484.8	(2.3)	496	72.8	(1.7)	123	[8]
12250.99	12292	−41	26.8	$4f^8(^7F)5d^26s\,^{10}F$	22.2	$4f^8(^7F)5d^26s\,^{10}D$	1.937		893.7	(1.7)	867	25.2	(7.3)	85	[10]
12645.32	12651	−6	66.1	$4f^8(^7F)5d6s^2\,^6H$	6.3	$4f^8(^7F)5d6s^2\,^6D$	0.984		607.4	(2.4)	636	433	(17)	631	[10]
12714.050	12751	−37	34.1	$4f^8(^7F)5d6s^2\,^6D$	26.2	$4f^8(^7F)5d6s^2\,^6P$	1.520		299.5	(1.0)	212	−308.5	(6.5)	−467	[10]
13277.23	13279	−2	27.5	$4f^8(^7F)5d^26s\,^8G$	12.4	$4f^8(^7F)5d^26s\,^8G$	1.531		464.5	(0.9)	477	921	(39)	960	[10]
13729.12	13715	15	31.4	$4f^8(^7F)5d^26s\,^{10}P$	19.6	$4f^8(^7F)5d^26s\,^{10}F$	1.868		538.8	(4.4)	524	−404	(29)	−392	[10]

Table 3. Continued.

E_{exp}	E_{calc}	ΔE	%	Main comp.	%	Sec. comp.	$g_{J_{calc}}$	$g_{J_{exp}}$	A_{exp}		A_{calc}	B_{exp}		B_{calc}	Ref.
$J = 9/2$															
1371.045	1328	43	31.1	$4f^8(^7F)5d6s^2\ ^8G$	29.2	$4f^8(^7F)5d6s^2\ ^8F$	1.546	1.541	602.219	(0.003)	613	1267.267	(0.030)	1269	[19]
2840.170	2859	−18	44.0	$4f^8(^7F)5d6s^2\ ^8G$	35.6	$4f^8(^7F)5d6s^2\ ^8D$	1.540	1.544	441.771	(0.005)	442	158.750	(0.040)	156	[19]
5829.860	5791	39	50.6	$4f^8(^7F)5d6s^2\ ^8F$	14.1	$4f^8(^7F)5d6s^2\ ^8P$	1.577	1.580	271.2	(0.7)	260	−349.8	(6.8)	−349	[10]
7441.030	7392	49	65.2	$4f^8(^7F)5d6s^2\ ^8H$	9.6	$4f^8(^7F)5d6s^2\ ^6G$	1.248	1.240	509.843	(0.003)	525	547.483	(0.003)	571	[21]
7824.190	7866	−42	59.3	$4f^8(^7F)5d6s^2\ ^6F$	10.9	$4f^8(^7F)5d6s^2\ ^6D$	1.411	1.433	621.5	(2.1)	634	789.8	(3.8)	797	[10]
8097.875	8121	−23	60.8	$4f^8(^7F)5d6s^2\ ^8P$	19.3	$4f^8(^7F)5d6s^2\ ^8D$	1.727	1.750	229.1	(1.7)	124	−398.8	(6.4)	−457	[10]
9145.230	9125	21	46.4	$4f^8(^7F)5d^26s\ ^{10}G$	19.4	$4f^8(^7F)5d^26s\ ^{10}F$	1.673	1.670	1069.3	(0.3)	1041	1088.8	(7.5)	1080	[9]
9897.730	9876	22	35.7	$4f^8(^7F)5d^26s\ ^{10}S$	21.8	$4f^8(^7F)5d^26s\ ^{10}P$	1.776	1.810	1109.4	(0.2)	1081	537.3	(3.7)	472	[9]
9986.73	9930	57	38.7	$4f^8(^7F)5d6s^2\ ^6G$	15.2	$4f^8(^7F)5d6s^2\ ^6D$	1.459		636.719	(0.003)	665	367.994	(0.003)	361	[21]
10680.17	10696	−16	48.9	$4f^8(^7F)5d6s^2\ ^6D$	19.2	$4f^8(^7F)5d6s^2\ ^6F$	1.473		351.9	(1.2)	337	−229.5	(7.8)	−302	[8]
11956.255	11945	11	71.6	$4f^8(^7F)5d6s^2\ ^6H$	6.7	$4f^8(^7F)5d6s^2\ ^8H$	1.105		576.1	(2.3)	544	945	(15)	937	[10]
12228.28	12263	−35	37.0	$4f^8(^7F)5d^26s\ ^{10}F$	15.6	$4f^8(^7F)5d^26s\ ^{10}D$	1.728		798.0	(1.5)	799	−277.1	(9.7)	−256	[10]
12776.31	12789	−12	29.5	$4f^8(^7F)5d^26s\ ^8G$	15.9	$4f^8(^7F)5d^26s\ ^8F$	1.469		414.7	(2.9)	430	864	(34)	862	[10]
13751.41	13792	−41	46.4	$4f^8(^7F)5d^26s\ ^{10}H$	28.3	$4f^8(^7F)5d^26s\ ^{10}I$	1.363		558.3	(1.5)	593	264.6	(7.6)	278	[10]
$J = 11/2$															
509.845	464	46	32.2	$4f^8(^7F)5d6s^2\ ^8G$	30.9	$4f^8(^7F)5d6s^2\ ^8F$	1.519	1.517	577.465	(0.002)	589	989.917	(0.030)	996	[19]
2310.090	2336	−26	45.4	$4f^8(^7F)5d6s^2\ ^8D$	40.6	$4f^8(^7F)5d6s^2\ ^8G$	1.528	1.530	405.106	(0.003)	390	−92.638	(0.050)	−62	[19]
5353.370	5337	16	49.9	$4f^8(^7F)5d6s^2\ ^8F$	21.3	$4f^8(^7F)5d6s^2\ ^8D$	1.533	1.545	267.2	(1.0)	245	−448.7	(9.8)	−484	[10]
6674.155	6682	−8	51.0	$4f^8(^7F)5d6s^2\ ^6F$	18.1	$4f^8(^7F)5d6s^2\ ^6G$	1.415	1.320	527.6	(1.2)	553	528.4	(1.4)	606	[10]
6988.820	6993	−5	60.6	$4f^8(^7F)5d6s^2\ ^8H$	17.7	$4f^8(^7F)5d6s^2\ ^6F$	1.330	1.315	446.7	(0.3)	476	739	(15)	697	[10]
8646.210	8633	13	53.6	$4f^8(^7F)5d^26s\ ^{10}G$	21.1	$4f^8(^7F)5d^26s\ ^{10}F$	1.586	1.600	984.255	(0.001)	979	925.956	(0.001)	931	[21]
8932.120	8920	12	52.9	$4f^8(^7F)5d6s^2\ ^6G$	14.8	$4f^8(^7F)5d6s^2\ ^6F$	1.346	1.470	456.1	(3.1)	476	589.1	(3.4)	549	[8]
10997.850	10969	29	70.0	$4f^8(^7F)5d6s^2\ ^6H$	9.7	$4f^8(^7F)5d6s^2\ ^8H$	1.225	1.210	500.3	(2.0)	484	1262.5	(2.5)	1157	[8]
11260.41	11308	−47	25.1	$4f^8(^7F)5d^26s\ ^{10}D$	20.1	$4f^8(^7F)5d^26s\ ^{10}P$	1.669	1.680	919.9	(2.3)	929	309	(13)	346	[10]
12453.14	12475	−22	28.9	$4f^8(^7F)5d^26s\ ^8G$	15.1	$4f^8(^7F)5d^26s\ ^8G$	1.475		370.011	(0.003)	379	660.165	(0.003)	658	[21]
13071.30	13083	−12	28.7	$4f^8(^7F)5d^26s\ ^{10}P$	27.2	$4f^8(^7F)5d^26s\ ^{10}H$	1.574		703.0	(3.8)	741	−203	(36)	−231	[10]
13666.46	13668	−2	20.8	$4f^8(^7F)5d^26s\ ^{10}I$	18.2	$4f^8(^7F)5d^26s\ ^{10}H$	1.528		635.0	(0.9)	648	−208	(36)	−238	[10]
… *57 levels* …															
25637.87	25641	−3	10.9	$4f^8(^7F)5d^26s\ ^4I$	7.2	$4f^8(^7F)5d^26s\ ^8F$	1.239	1.334			570			354	
… *8 levels* …															
26553.26	26643	−90	20.4	$4f^8(^7F)5d^26s\ ^6F$	9.2	$4f^9(^6F)6s6p\ ^4G$	1.376				491			401	

Table 3. Continued.

E_{exp}	E_{calc}	ΔE	%	Main comp.	%	Sec. comp.	$g_{J_{\mathrm{calc}}}$	$g_{J_{\mathrm{exp}}}$	A_{exp}		A_{calc}	B_{exp}		B_{calc}	Ref.
$J = 13/2$															
285.500	275	11	59.0	4f^{8}(^{7}F)5d6s^{2} ^{8}G	24.9	4f^{8}(^{7}F)5d6s^{2} ^{8}F	1.466	1.464	532.204	(0.002)	542	928.861	(0.020)	900	[19]
3719.705	3678	42	64.8	4f^{8}(^{7}F)5d6s^{2} ^{8}F	21.9	4f^{8}(^{7}F)5d6s^{2} ^{8}G	1.504	1.505	354.454	(0.003)	320	72.183	(0.030)	28	[19]
6351.750	6315	37	68.3	4f^{8}(^{7}F)5d6s^{2} ^{8}H	10.3	4f^{8}(^{7}F)5d6s^{2} ^{6}G	1.355	1.350	438.5	(2.2)	441	1122	(29)	1145	[10]
7059.900	7072	−12	63.0	4f^{8}(^{7}F)5d6s^{2} ^{6}G	11.8	4f^{8}(^{7}F)5d6s^{2} ^{6}H	1.369	1.380	519.5	(0.7)	544	1179.7	(2.7)	1198	[10]
8277.040	8273	4	56.7	4f^{8}(^{7}F)5d^{2}6s ^{10}G	19.1	4f^{8}(^{7}F)5d^{2}6s ^{10}F	1.555	1.570	981.2	(2.6)	993	820	(24)	794	[10]
9763.020	9789	−26	69.7	4f^{8}(^{7}F)5d6s^{2} ^{6}H	12.3	4f^{8}(^{7}F)5d6s^{2} ^{8}H	1.297	1.300	469.4	(0.8)	442	1480	(11)	1505	[10]
11425.94	11419	7	31.8	4f^{8}(^{7}F)5d^{2}6s ^{10}F	11.8	4f^{8}(^{7}F)5d^{2}6s ^{10}D	1.569		672.5	(0.4)	705	75.4	(9.9)	49	[10]
12475.74	12468	8	25.3	4f^{8}(^{7}F)5d^{2}6s ^{8}G	16.4	4f^{8}(^{7}F)5d^{2}6s ^{10}D	1.505		439.3	(2.1)	458	529	(26)	612	[10]
12906.60	12859	47	45.1	4f^{8}(^{7}F)5d^{2}6s ^{10}D	20.9	4f^{8}(^{7}F)5d^{2}6s ^{10}H	1.555		831.0	(1.1)	839	820	(17)	884	[10]
13116.48	13136	−20	21.6	4f^{8}(^{7}F)5d^{2}6s ^{10}D	19.6	4f^{8}(^{7}F)5d^{2}6s ^{10}I	1.512		836.6	(0.8)	765	704	(15)	599	[10]
… *6 levels* …															
17875.98	17858	18	35.4	4f^{8}(^{7}F)5d^{2}6s ^{8}I	13.2	4f^{8}(^{7}F)5d^{2}6s ^{8}H	1.285				446			483	
… *24 levels* …															
23043.43	23011	32	11.1	4f^{8}(^{7}F)5d^{2}6s ^{6}H	8.8	4f^{8}(^{7}F)5d^{2}6s ^{8}F	1.348	1.391	685.7	(2.0)	639	915	(24)	591	[22]
	23133		20.6	4f^{8}(^{7}F)5d^{2}6s ^{8}G	8.1	4f^{8}(^{7}F)5d^{2}6s ^{6}G	1.380				593			576	
23147.92	23172	−24	13.6	4f^{8}(^{7}F)5d^{2}6s ^{8}F	10.7	4f^{9}(^{6}H)6s6p ^{4}I	1.349	1.339	708.9	(0.6)	767	1328	(29)	875	[22]
… *10 levels* …															
25373.85	25336	38	15.2	4f^{8}(^{7}F)5d^{2}6s ^{8}I	10.3	4f^{8}(^{7}F)5d^{2}6s ^{8}H	1.348	1.354			674			553	
	25445		11.6	4f^{8}(^{7}F)5d^{2}6s ^{8}F	9.3	4f^{9}(^{6}H)6s6p ^{6}H	1.348				645			416	
25553.46	25565	−11	19.0	4f^{9}(^{6}H)6s6p ^{6}H	9.4	4f^{8}(^{7}F)5d^{2}6s ^{8}F	1.381	1.328			501			305	
	25616		12.2	4f^{8}(^{5}L)5d6s^{2} ^{6}M	8.1	4f^{8}(^{5}G)5d6s^{2} ^{6}G	1.180				802			126	
25717.68	25710	8	16.5	4f^{9}(^{6}F)6s6p ^{8}F	6.0	4f^{8}(^{7}F)5d^{2}6s ^{6}H	1.325	1.300			529			281	
… *6 levels* …															
26592.90	26611	−19	24.1	4f^{8}(^{7}F)5d^{3} ^{10}F	15.7	4f^{8}(^{7}F)5d^{3} ^{10}G	1.566				−820			308	
	26767		34.2	4f^{8}(^{5}L)5d6s^{2} ^{6}K	8.4	4f^{8}(^{5}L)5d6s^{2} ^{6}I	1.117				1003			723	
$J = 15/2$															
462.080	530	−68	85.4	4f^{8}(^{7}F)5d6s^{2} ^{8}G	4.2	4f^{8}(^{7}F)5d6s^{2} ^{8}H	1.456	1.456	472.643	(0.002)	474	1154.239	(0.017)	1148	[19]
5425.060	5442	−17	64.6	4f^{8}(^{7}F)5d6s^{2} ^{8}H	20.3	4f^{8}(^{7}F)5d6s^{2} ^{6}H	1.374	1.370	459.627	(0.003)	471	1724.243	(0.003)	1728	[20]
7767.015	7794	−27	66.8	4f^{8}(^{7}F)5d6s^{2} ^{6}H	21.6	4f^{8}(^{7}F)5d6s^{2} ^{8}H	1.343	1.342	509.0	(0.9)	498	2048	(15)	2063	[10]
8190.465	8193	−3	62.4	4f^{8}(^{7}F)5d^{2}6s ^{10}G	13.2	4f^{8}(^{7}F)5d^{2}6s ^{10}F	1.532	1.540	948.5	(1.1)	973	699	(31)	653	[10]
11580.68	11570	11	43.2	4f^{8}(^{7}F)5d^{2}6s ^{10}F	15.3	4f^{8}(^{7}F)5d^{2}6s ^{10}H	1.522		615.3	(1.8)	604	155	(29)	77	[10]
12628.67	12639	−11	28.9	4f^{8}(^{7}F)5d^{2}6s ^{10}H	28.0	4f^{8}(^{7}F)5d^{2}6s ^{10}I	1.452		654.4	(0.3)	653	427	(38)	474	[10]

Table 3. Continued.

E_{exp}	E_{calc}	ΔE	%	Main comp.	%	Sec. comp.	$g_{J_{\mathrm{calc}}}$	$g_{J_{\mathrm{exp}}}$	A_{exp}		A_{calc}	B_{exp}		B_{calc}	Ref.
12932.66	12905	28	32.0	$4f^8(^7F)5d^26s\ ^8G$	17.6	$4f^8(^7F)5d^26s\ ^8G$	1.473		294.2	(1.8)	294	406	(24)	343	[10]
14569.67	14610	−40	41.9	$4f^8(^7F)5d^26s\ ^{10}I$	30.8	$4f^8(^7F)5d^26s\ ^{10}H$	1.398		566.0	(3.4)	600	294	(31)	266	[10]
14888.11	14890	−2	41.7	$4f^9(^6H)6s6p\ ^8G$	18.5	$4f^9(^6H)6s6p\ ^8H$	1.396	1.391			940			1398	
15387.79	15341	47	30.7	$4f^8(^7F)5d^26s\ ^8H$	15.1	$4f^8(^7F)5d^26s\ ^8I$	1.367	1.367	525.7	(0.4)	458	1080.0	(5.9)	1122	[10]
16343.30	16340	3	28.6	$4f^9(^6H)6s6p\ ^4I$	18.6	$4f^9(^6H)6s6p\ ^8G$	1.284	1.397			193			1456	
16431.13	16452	−21	62.8	$4f^8(^7F)5d^26s\ ^{10}G$	12.1	$4f^8(^7F)5d^26s\ ^{10}G$	1.516	1.460			793			1019	
… *8 levels* …															
19920.41	19953	−33	17.1	$4f^8(^7F)5d^26s\ ^8G$	14.1	$4f^8(^7F)5d^26s\ ^8H$	1.410				992			708	
… *9 levels* …															
23112.35	23011	102	20.9	$4f^9(^6H)6s6p\ ^6I$	18.4	$4f^9(^6H)6s6p\ ^8I$	1.303		968.0	(0.1)	1037	916.9	(1.3)	1233	[22]
23031.84	23114	−82	9.5	$4f^8(^5G)5d6s^2\ ^6H$	9.4	$4f^8(^5G)5d6s^2\ ^6H$	1.327	1.240	880.9	(0.6)	832	838.3	(4.5)	812	[22]
… *11 levels* …															
25825.53	25836	−11	21.0	$4f^8(^5L)5d6s^2\ ^6K$	8.4	$4f^9(^6H)6s6p\ ^6I$	1.219	1.246			869			827	
$J = 17/2$															
4646.830	4638	9	89.5	$4f^8(^7F)5d6s^2\ ^8H$	2.7	$4f^8(^7F)5d^3\ ^8H$	1.406	1.406	481.738	(0.002)	451	2245.914	(0.050)	2228	[19]
8506.710	8504	2	73.2	$4f^8(^7F)5d^26s\ ^{10}G$	11.8	$4f^8(^7F)5d^26s\ ^{10}G$	1.518	1.530	915.3	(0.5)	937	464	(37)	408	[10]
11879.20	11900	−21	47.3	$4f^8(^7F)5d^26s\ ^{10}H$	31.3	$4f^8(^7F)5d^26s\ ^{10}I$	1.438	1.430	757.6	(0.4)	762	1167	(24)	1158	[10]
14016.91	14033	−16	38.4	$4f^8(^7F)5d^26s\ ^{10}I$	30.0	$4f^8(^7F)5d^26s\ ^{10}H$	1.415		648.9	(2.3)	662	669.5	(3.5)	758	[10]
14718.11	14704	15	46.2	$4f^8(^7F)5d^26s\ ^8H$	15.6	$4f^8(^7F)5d^26s\ ^{10}I$	1.397	1.400	781.5	(4.9)	617	1020	(18)	1103	[10]
15189.26	15190	−1	46.2	$4f^9(^6H)6s6p\ ^8H$	11.9	$4f^9(^6H)6s6p\ ^8I$	1.369	1.409	1025.6	(0.7)	995	682	(29)	773	[10]
	15678		61.3	$4f^8(^7F)5d^26s\ ^{10}G$	16.0	$4f^8(^7F)5d^26s\ ^{10}G$	1.496				863			1079	
	16733		32.2	$4f^8(^7F)5d^26s\ ^8I$	18.8	$4f^8(^7F)5d^26s\ ^8H$	1.360				432			1080	
17249.59	17245	5	46.4	$4f^9(^6H)6s6p\ ^6I$	25.1	$4f^9(^6H)6s6p\ ^8H$	1.324		857.1	(0.4)	866	1758.9	(5.0)	1688	[10]
… *9 levels* …															
23107.25	23128	−20	25.2	$4f^8(^7F)5d^26s\ ^8I$	22.9	$4f^8(^7F)5d^26s\ ^8H$	1.357	1.289			758			1386	
$J = 19/2$															
11331.14	11330	1	65.9	$4f^8(^7F)5d^26s\ ^{10}H$	28.4	$4f^8(^7F)5d^26s\ ^{10}I$	1.451	1.460	876.3	(3.8)	890	1460	(20)	1469	[10]
13398.40	13397	2	56.8	$4f^8(^7F)5d^26s\ ^{10}I$	27.2	$4f^8(^7F)5d^26s\ ^{10}H$	1.421		690.6	(0.6)	687	1023	(16)	1027	[10]
$J = 21/2$															
12283.30	12248	36	95.1	$4f^8(^7F)5d^26s\ ^{10}I$	2.1	$4f^8(^5G)5d^26s\ ^8K$	1.425		845.9	(0.1)	855	1906	(11)	1927	[10]

Table 4. Comparison of the experimental and calculated hfs A and B constants (MHz) of the even-parity levels obtained in full and limited number of 4f^8 and 4f^9-core states, respectively.

$E_{\rm exp}$	A				B			
	Experiment		This work	[10]	Experiment		This work	[10]
$J = 1/2$								
4018.210	2584.8	(4.0)	2591	2566				
6259.090	−1762.5	(8.9)	−1797	−1759				
$J = 3/2$								
3705.820	883.905	(0.030)	884	883	−15.510	(0.250)	−16	−8
5483.980	−177.8	(7.6)	−159	−131	−504	(23)	−518	−533
6849.720	−755.3	(5.2)	−749	−792	281	(16)	325	300
8336.310	1645.9	(4.5)	1644	1652	744	(25)	778	774
10920.180	1001.8	(3.2)	1001	1047	−133	(19)	−123	−121
$J = 5/2$								
3174.575	652.766	(0.020)	652	652	267.611	(0.150)	267	279
4695.505	215.653	(0.015)	211	224	−401.862	(0.060)	−420	−429
6801.190	−123.7	(2.8)	−113	−131	−286	(15)	−290	−310
8130.680	874.4	(4.8)	875	872	411	(25)	433	425
10030.350	783.5	(0.1)	737	769	515.4	(9.7)	546	585
10456.670	912.9	(6.9)	907	907	149	(35)	105	97
12296.45	332.6	(0.4)	288	315	−52	(24)	−26	−55
$J = 7/2$								
2419.480	591.564	(0.007)	588	588	733.233	(0.070)	721	746
3819.850	358.918	(0.007)	355	357	−140.881	(0.050)	−157	−170
6488.280	114.9	(0.3)	116	112	−498.7	(0.7)	−531	−540
7839.850	606.2	(0.7)	623	615	429.7	(0.4)	419	406
8994.660	710.991	(0.003)	696	712	966.850	(0.003)	987	1000
9867.650	903.5	(2.5)	898	887	533	(23)	483	469
10324.740	−35.1	(2.0)	−16	−7	−563.3	(8.5)	−393	−582
11107.07	484.8	(2.3)	496	489	72.8	(1.7)	123	143
12250.99	893.7	(1.7)	867	861	25.2	(7.3)	85	93
12645.32	607.4	(2.4)	636	668	433	(17)	631	633
12714.050	299.5	(1.0)	212	274	−308.5	(6.5)	−467	−394
13277.23	464.5	(0.9)	477	467	921	(39)	960	960
13729.12	538.8	(4.4)	524	487	−404	(29)	−392	−378
$J = 9/2$								
1371.045	602.219	(0.003)	613	602	1267.267	(0.030)	1269	1290
2840.170	441.771	(0.005)	442	434	158.750	(0.040)	156	149
5829.860	271.2	(0.7)	260	265	−349.8	(6.8)	−349	−351
7441.030	509.843	(0.003)	525	516	547.483	(0.003)	571	540
7824.190	621.5	(2.1)	634	633	789.8	(3.8)	797	790
8097.875	229.1	(1.7)	124	207	−398.8	(6.4)	−457	−441
9145.230	1069.3	(0.3)	1041	1041	1088.8	(7.5)	1080	1045
9897.730	1109.4	(0.2)	1081	1162	537.3	(3.7)	472	518
9986.73	636.719	(0.003)	665	638	367.994	(0.003)	361	220
10680.17	351.9	(1.2)	337	354	−229.5	(7.8)	−302	−276
11956.255	576.1	(2.3)	544	583	945	(15)	937	975
12228.28	798.0	(1.5)	799	798	−277.1	(9.7)	−256	−268
12776.31	414.7	(2.9)	430	408	864	(34)	862	867
13751.41	558.3	(1.5)	593	555	264.6	(7.6)	278	271

Table 4. Continued.

E_{exp}	A				B			
	Experiment		This work	[10]	Experiment		This work	[10]
$J = 11/2$								
509.845	577.465	(0.002)	589	579	989.917	(0.030)	996	1008
2310.090	405.106	(0.003)	390	398	−92.638	(0.050)	−62	−96
5353.370	267.2	(1.0)	245	265	−448.7	(9.8)	−484	−476
6674.155	527.6	(1.2)	553	539	528.4	(1.4)	606	545
6988.820	446.7	(0.3)	476	457	739	(15)	697	708
8646.210	984.255	(0.001)	979	977	925.956	(0.001)	931	913
8932.120	456.1	(3.1)	476	472	589.1	(3.4)	549	584
10997.850	500.3	(2.0)	484	511	1262.5	(2.5)	1157	1188
11260.41	919.9	(2.3)	929	920	309	(13)	346	349
12453.14	370.011	(0.003)	379	371	660.165	(0.003)	658	645
13071.30	703.0	(3.8)	741	726	−203	(36)	−231	−214
13666.46	635.0	(0.9)	648	638	−208	(36)	−238	−253
$J = 13/2$								
285.500	532.204	(0.002)	542	532	928.861	(0.020)	900	932
3719.705	354.454	(0.003)	320	346	72.183	(0.030)	28	47
6351.750	438.5	(2.2)	441	441	1122	(29)	1145	1118
7059.900	519.5	(0.7)	544	535	1179.7	(2.7)	1198	1221
8277.040	981.2	(2.6)	993	995	820	(24)	794	778
9763.020	469.4	(0.8)	442	473	1480	(11)	1505	1546
11425.94	672.5	(0.4)	705	708	75.4	(9.9)	49	62
12475.74	439.3	(2.1)	458	489	529	(26)	612	638
12906.60	831.0	(1.1)	839	803	820	(17)	884	820
13116.48	836.6	(0.8)	765	752	704	(15)	599	557
23043.43	685.7	(2.0)	639		915	(24)	591	
23147.92	708.9	(0.6)	767		1328	(29)	875	
$J = 15/2$								
462.080	472.643	(0.002)	474	470	1154.239	(0.017)	1148	1144
5425.060	459.627	(0.003)	471	466	1724.243	(0.003)	1728	1721
7767.015	509.0	(0.9)	498	517	2048	(15)	2063	2114
8190.465	948.5	(1.1)	973	978	699	(31)	653	646
11580.68	615.3	(1.8)	604	602	155	(29)	77	104
12628.67	654.4	(0.3)	653	648	427	(38)	474	388
12932.66	294.2	(1.8)	294	303	406	(24)	343	371
14569.67	566.0	(3.4)	600	559	294	(31)	266	260
15387.79	525.7	(0.4)	458	545	1080.0	(5.9)	1122	1206
23112.35	968.0	(0.1)	1037		916.9	(1.3)	1233	
23031.84	880.9	(0.6)	832		838.3	(4.5)	812	
$J = 17/2$								
4646.830	481.738	(0.002)	451	481	2245.914	(0.050)	2228	2195
8506.710	915.3	(0.5)	937	940	464	(37)	408	393
11879.20	757.6	(0.4)	762	758	1167	(24)	1158	1132
14016.91	648.9	(2.3)	662	636	669.5	(3.5)	758	735
14718.11	781.5	(4.9)	617	785	1020	(18)	1103	881
15189.26	1025.6	(0.7)	995	1019	682	(29)	773	693
17249.59	857.1	(0.4)	866	871	1758.0	(5.0)	1688	1929
$J = 19/2$								
11331.14	876.3	(3.8)	890	899	1460	(20)	1469	1431
13398.40	690.6	(0.6)	687	676	1023	(16)	1027	1003
$J = 21/2$								
12283.30	845.9	(0.1)	855	859	1906	(11)	1927	1880

Table 5. Values of the one- and two-body hyperfine structure parameters (MHz) and effective radial integrals (a.u.) obtained from the experimental data for the even parity configurations of Tb I; OHFS stands for "optimized Hartree-Fock-Slater" method.

Parameter	Value		Comments
Magnetic-dipole hfs interactions			
$a_{4f}^{01} = a_{4f}^{12}$	1072	(26)	fitted
$a_{5d}^{01} = a_{5d}^{12}$	264	(58)	fitted
a_{6s}^{10}	11206	(501)	fitted
Configuration $4f^8 5d^3$ and $4f^8 5d^2 6s$			
$E^3(n_0s4f,4f6s)\ P^{10}(n_0s,6s)$	−3334	(850)	fitted, $n_0 = 1,\ldots,5$
$E^3(n_0s4f,4fn's)\ P^{10}(n_0s,n's)$	−720	(190)	fixed, $n_0 = 1,2,\ldots,5,\ n' = 6,7,8,\ldots$
$E^2(n_0s5d,5d6s)\ P^{10}(n_0s,6s)$	−10540	(910)	fitted, $n_0 = 1,\ldots,5$
$E^2(n_0s5d,5dn's)\ P^{10}(n_0s,n's)$	−2277	(200)	fixed, $n_0 = 1,2,\ldots,5,\ n' = 6,7,8,\ldots$
$R^0(4f4f,4fn'f)\ P^{01}(4f,n'f)$	8	(3)	fitted,$n' = 5,6,7,\ldots$
$R^0(4f4f,4fn'f)\ P^{12}(4f,n'f)$	−75	(7)	fitted, $n' = 5,6,7,\ldots$
$D^0(n_0d6s,5d6s)\ P^{01}(n_0d,5d) =$			
$D^0(n_0d6s,5d6s)\ P^{12}(n_0d,5d)$	47	(14)	fitted, $n_0 = 3,4$
$E^2(n_0d6s,6s5d)\ P^{01}(n_0d,5d) =$			
$E^2(n_0d6s,6s5d)\ P^{12}(n_0d,5d)$	17	(8)	fitted, $n_0 = 3,4$
$D^0(n_0d4f,5d4f)\ P^{01}(n_0d,5d) =$			
$D^0(n_0d4f,5d4f)\ P^{12}(n_0d,5d)$	3	(1)	fitted, $n_0 = 3,4$
$D^2(n_0d4f,5d4f)\ P^{01}(n_0d,5d) =$			
$D^2(n_0d4f,5d4f)\ P^{12}(n_0d,5d)$	−193	(31)	fitted, $n_0 = 3,4$
$E^1(n_0d4f,4f5d)\ P^{01}(n_0d,5d) =$			
$E^1(n_0d4f,4f5d)\ P^{12}(n_0d,5d)$	14	(8)	fitted, $n_0 = 3,4$
Configuration $4f^8 5d6s^2$			
$E^2(n_0s5d,5dn's)\ P^{10}(n_0s,n's)$	−1281	(120)	fitted, $n_0 = 1,2,\ldots,6,\ n' = 7,8,\ldots$
$E^3(n_0s4f,4fn's)\ P^{10}(n_0s,n's)$	1229	(94)	fitted, $n_0 = 1,2,\ldots,6,\ n' = 7,8,\ldots$
Configuration $4f^9 6s6p$			
$a_{6p}^{01} = a_{6p}^{12}$	528	(116)	fixed
$E^1(n_0s6p,6pn's)\ P^{10}(n_0s,n's)$	−5503	(550)	fitted, $n_0 = 1,2,\ldots,5,\ n' = 7,8,\ldots$
Inter-configuration interaction			
a_{5d6s}^{12}	1307	(180)	fitted
$D^2(n_0s5d,5d5d)\ P^{10}(n_0s,6s)$	−24037	(1700)	fitted, $n_0 = 1,\ldots,5$
$\langle r^{-3}\rangle_{4f\,\text{non-rel}}$	8.368		this work
	8.962		(HF) [30]
	8.997		(OHFS) [30]
$\langle r^{-3}\rangle_{4f}^{01}$	8.311		(exp for $4f^8 5d6s^2$ configuration) [29]
	8.1		(exp for $4f^8 5d6s^2$ configuration) [8]
	8.344		(OHFS) [30]
$\langle r^{-3}\rangle_{4f}^{12}$	9.549		(exp for $4f^8 5d6s^2$ configuration) [29]
	8.7		(exp for $4f^8 5d6s^2$ configuration) [8]
	9.066		(OHFS) [30]
$\langle r^{-3}\rangle_{5d\,\text{non-rel}}$	2.779		this work
$\langle r^{-3}\rangle_{5d}^{01}$	2.89		(exp for $4f^8 5d6s^2$ configuration) [29]
	3.1		(exp for $4f^8 5d6s^2$ configuration) [8]
$\langle r^{-3}\rangle_{5d}^{12}$	1.13		(exp for $4f^8 5d6s^2$ configuration) [29]
	0.9		(exp for $4f^8 5d6s^2$ configuration) [8]
$\langle r^{-3}\rangle_{6s\,\text{eff}}^{10}$	131.207		this work

Table 5. Continued.

Parameter	Value		Comments
Electric-quadrupole hfs interactions			
b_{4f}^{02}	2235	(40)	fitted
b_{4f}^{13}	718	(140)	fitted
b_{4f}^{11}	−259	(74)	fitted
b_{5d}^{02}	962	(40)	fitted
b_{5d}^{13}	615	(95)	fitted
b_{5d}^{11}	−419	(61)	fitted
R^0(4f4f,4fn'f) P^{02}(4f,n'f)	−177	(31)	fitted, $n' = 5, 6, 7, \ldots$
E^2(n_0d6s,6s5d) P^{02}(n_0d,5d)	−136	(20)	fitted, $n_0 = 3, 4$
D^0(n_0d4f,5d4f) P^{02}(n_0d,5d)	20	(6)	fitted, $n_0 = 3, 4$
E^1(n_0d4f,4f5d) P^{02}(n_0d,5d)	87	(37)	fitted, $n_0 = 3, 4$
$b_{5d,6s}^{02}$	−1599	(220)	fitted
$\langle r^{-3}\rangle_{4f\,\mathrm{eff}}^{02}$	6.643		this work
$\langle r^{-3}\rangle_{4f}^{02}$	6.946		(exp for $4f^8 5d 6s^2$ configuration) [29]
	6.7		(exp for $4f^8 5d 6s^2$ configuration) [8]
	6.458		(exp for $4f^9 6s^2$ configuration) [29]
	8.365		(OHFS) [30]
$\langle r^{-3}\rangle_{4f}^{11}$	−0.770		this work
	−0.562		(exp for $4f^8 5d 6s^2$ configuration) [29]
	−1.7		(exp for $4f^8 5d 6s^2$ configuration) [8]
	−0.461		(OHFS) [30]
$\langle r^{-3}\rangle_{4f}^{13}$	2.134		this work
	0.27		(exp for $4f^8 5d 6s^2$ configuration) [29]
	4.2		(exp for $4f^8 5d 6s^2$ configuration) [8]
	1.003		(OHFS) [30]
$\langle r^{-3}\rangle_{5d\,\mathrm{eff}}^{02}$	2.859		this work
$\langle r^{-3}\rangle_{5d}^{02}$	3.733		(exp for $4f^8 5d 6s^2$ configuration) [29]
	3.7		(exp for $4f^8 5d 6s^2$ configuration) [8]

The configuration interaction effects concerning the excitation of electrons from the closed $\mathrm{n_0}$s shells to the open 6s-shell or to empty n's shells are different in each of the considered configurations and were included by the following intra-configuration parameters: E^3(n_0s4f,4f6s) P^{10}(n_0s,6s), E^3(n_0s4f,4fn's) P^{10}(n_0s,n's), E^2(n_0s5d,5d6s) P^{10}(n_0s,6s), E^2(n_0s5d,5dn's) P^{10}(n_0s,n's), E^1(n_0s6p,6pn's) P^{10}(n_0s,n's) and inter-configuration parameter D^2(n_0s5d,5d5d) P^{10}(n_0s,6s). The precise description of above parameters and their significance were included in the papers [6, 10, 25].

The value of radial integral $\langle r^{-3}\rangle_{6s\,\mathrm{eff}}^{10} = 131.207$ a.u. obtained within this work compared to the value (105.284 a.u.) published earlier [10] agrees better with the monotonic increase trend with the atomic number proposed by Pfeufer [29] for some selected one-electron radial integrals of various elements along the lanthanides series.

The ratios of two-body hfs radial parameters describing magnetic dipole and electric quadrupole interactions should be identical. On the basis of results of performed parameterization (see table 5) we obtain

E^2(n_0d6s,6s5d) P^{01}(n_0d,5d)/E^2(n_0d6s,6s5d) P^{02}(n_0d,5d) $= -0.13$,
D^0(n_0d4f,5d4f) P^{01}(n_0d,5d)/D^0(n_0d4f,5d4f) P^{02}(n_0d,5d) $= 0.15$,
E^1(n_0d4f,4f5d) P^{01}(n_0d,5d)/E^1(n_0d4f,4f5d) P^{02}(n_0d,5d) $= 0.16$.

This points out that contributions originating from the second-order perturbation theory within the frame of magnetic dipole or electric quadrupole interactions in the hyperfine structure is not fully correct. The more precise measurements of the hyperfine splittings would be required.

4 Conclusions

By extending the fine- and hyperfine analysis to the complete set of $4f^N$-core states we got improved agreement between the calculated and experimental energy level values as well as calculated and experimental hyperfine structure constants A and B. Based on our results, we can assume that the description of the electronic levels is more reliable. Therefore, we conclude that our earlier semi-empirical analysis of the rare-earth spectra related to the americium, europium and praseodymium atoms [31–34] should be repeated. Also, the extensive investigations of the hyperfine structure of the terbium atom with the method of laser induced fluorescence in a hollow cathode discharge, carried out in our experimental group, provided a lot of new data for odd parity levels [35]. This motivated us to work intensively on the development of novelty kind of computational procedures optimization for both the generation of angular coefficients of such huge energy matrix and diagonalization problem. This work shows that we have created an effective tool for precise determination of attributes of an atom, such as the energy levels, as well as the energy sublevels of the hyperfine structure, having a number of valence electrons, which can occur in all provided by quantum mechanics configurations.

We express our gratitude to Agnieszka Łastowska (Microsoft Poland) for her support and assistance. This work was performed in the framework of Microsoft Azure for Research grant awarded to Andrzej Sikorski. This work was partially supported by the Research Projects of the Polish Ministry of Sciences and Higher Education: 06/65/DSPB/5173 (ME) and 04/45/DSPB/0162 (JR and JD).

References

1. M. Elantkowska, J. Ruczkowski, J. Dembczyński, Eur. Phys. J. Plus **130**, 14 (2015).
2. M. Elantkowska, J. Ruczkowski, J. Dembczyński, Eur. Phys. J. Plus **130**, 15 (2015).
3. M. Elantkowska, J. Ruczkowski, J. Dembczyński, Eur. Phys. J. Plus **130**, 83 (2015).
4. M. Elantkowska, J. Ruczkowski, J. Dembczyński, Eur. Phys. J. Plus **130**, 170 (2015).
5. M. Elantkowska, J. Ruczkowski, J. Dembczyński, Eur. Phys. J. Plus **131**, 47 (2016).
6. M. Elantkowska, J. Ruczkowski, J. Dembczyński, Eur. Phys. J. Plus **131**, 429 (2016).
7. M. Elantkowska, A. Sikorski, J. Ruczkowski, J. Dembczyński, Eur. Phys. J. Plus **132**, 134 (2017).
8. B. Furmann, D. Stefanska, A. Krzykowski, Spectrochim. Acta, Part B **111**, 38 (2015).
9. B. Furmann, D. Stefanska, A. Krzykowski, J. Phys. B **49**, 025001 (2016).
10. D. Stefanska, M. Elantkowska, J. Ruczkowski, B. Furmann, J. Quantum Spectrosc. Radiat. Transf. **189**, 441 (2017).
11. D. Stefanska, M. Suski, B. Furmann, Laser Phys. Lett. **14**, 045701 (2017).
12. K. Rajnak, B.G. Wybourne, Phys. Rev. **132**, 280 (1963).
13. S. Feneuille, J. Phys. France **28**, 497 (1967).
14. J. Dembczyński, G. Szawioła, M. Elantkowska, E. Stachowska, J. Ruczkowski, Phys. Scr. **54**, 444 (1996).
15. R.D. Cowan, *The Theory of Atomic Structure and Spectra* (Berkeley University of California Press, Berkeley, 1981).
16. R.D. Cowan, *Robert D. Cowan's Atomic Structure Code*, `https://www.tcd.ie/Physics/people/Cormac.McGuinness/Cowan/`.
17. A. Kramida, Yu. Ralchenko, J. Reader, NIST ASD Team, *NIST Atomic Spectra Database* (ver. 5.3), available at `http://physics.nist.gov/asd` (National Institute of Standards and Technology, Gaithersburg, MD, 2017).
18. W.C. Martin, R. Zalubas, L. Hagan, *Atomic energy levels – The rare-earth elements*, in Nat. Stand. Ref. Data Ser., NSRDS-NBS 60, Nat. Bur. Stand., U.S., 1978.
19. W.J. Childs, Phys. Rev. A **2**, 316 (1970).
20. W.J. Childs, L.S. Goodman, J. Opt. Soc. Am. **69**, 815 (1979).
21. W.J. Childs, J. Opt. Soc. Am. B **9**, 191 (1992).
22. D. Stefanska, B. Furmann, private communication.
23. P.G.H. Sandars, J. Beck, Proc. R. Soc. A **289**, 97 (1965).
24. W. Nowak, J. Karwowski, J. Dembczyński, J. Phys. France **45**, 681 (1984).
25. J. Dembczyński, M. Elantkowska, B. Furmann, J. Ruczkowski, D. Stefańska, J. Phys. B: At. Mol. Opt. Phys. **43**, 065001 (2010).
26. S. Feneuille, L. Armstrong Jr., Phys. Rev. A **8**, 1173 (1973).
27. L. Armstrong Jr., *Theory of the Hyperfine Structure of Free Atoms* (Willey-Interscience, New York, 1971).
28. I. Lindgren, J. Morrison, *Atomic Many-Body Theory* (Springer-Verlag, Berlin Heidelberg New York, 1982).
29. V. Pfeufer, Z. Phys. D **4**, 351 (1987).
30. I. Lindgren, A. Rosén, in *Case Studies in Atomic Physics*, edited by E. McDaniel, M. McDowell (Elsevier, 1975) pp. 93–196, `https://doi.org/http://dx.doi.org/10.1016/B978-0-7204-0331-2.50007-X`.

31. J. Dembczyński, M. Elantkowska, K. Bekk, H. Rebel, M. Wilson, Z. Phys. D **13**, 181 (1989).
32. M. Elantkowska, A. Bernard, J. Dembczyński, J. Ruczkowski, Z. Phys. D **27**, 103 (1993).
33. E. Stachowska, M. Elantkowska, J. Ruczkowski, J. Dembczyński, Phys. Scr. **65**, 237 (2002).
34. J. Ruczkowski, E. Stachowska, M. Elantkowska, G.H. Guthöhrlein, J. Dembczyński, Phys. Scr. **68**, 133 (2003).
35. D. Stefanska, B. Furmann, J. Phys. B: At. Mol. Opt. Phys. **50**, 175002 (2017).